Electronic Supplementary Material (ESI) for Physical Chemistry Chemical Physics.

Electronic Supporting Information

Physical and chemical properties and degradation of $MAPbBr_3$ films on transparent substrates

Valentina Carpenella[1‡], *Fabrizio Messina*[2‡], *Jessica Barichello*[3], *Fabio Matteocci*[3], *Paolo Postorino*[4], *Caterina Petrillo*[5], *Alessandro Nucara*[4,6], *Danilo Dini*[2], *and Claudia Fasolato*[7*]

[1] Department of Science, University of Roma Tre, Via della Vasca Navale 84, 00146 Rome, Italy

[2] Department of Chemistry, Sapienza University of Rome, P.le A. Moro 5, 00185 Rome, Italy

[3] CHOSE, Department of Electronic Engineering, University of Rome Tor Vergata, Rome, 00133 Italy

[4] Department of Physics, Sapienza University of Rome, Piazzale Aldo Moro 5, 00185 Rome, Italy

[5] Department of Physics and Geology, University of Perugia, Via A. Pascoli, 06123, Perugia, Italy

[6] CNR-SPIN, c/o Sapienza University of Rome, Piazzale Aldo Moro 5, 00185 Rome, Italy

[7] CNR-ISC, Istituto dei Sistemi Complessi, c/o Sapienza University of Rome, P.le A. Moro 5, 00185 Rome, Italy

*Corresponding Author: claudia.fasolato@cnr.it

‡These authors contributed equally

S1 Absorption spectra and background subtraction

In Figure S1, we show the average spectra obtained from the data shown in Figure 1(a-d) before the background subtraction. It is evident that the spectra of the films obtained from the 1.4 M precursor concentrations feature a much more pronounced scattering background, well visible as a smooth contribution to the optical extinction even below the bandgap edge (*i.e.*, at wavelengths larger than 530 nm). In general, one can expect that such scattering contribution originates from the granular nature of the thin films; more specifically, the characteristic wrinkling of the samples obtained at higher precursor concentration (1.4 M), which are the thicker ones (thickness > 200 nm), produces modulations in the sample density and surface morphology on a scale in the order of the wavelength of visible light, thus enhancing the elastic scattering of light traveling through the sample. To estimate the thickness of the films from the optical absorption data (Figure 2 in the main text), we have subtracted the scattering background in the form of a smooth polynomial function (2nd order).

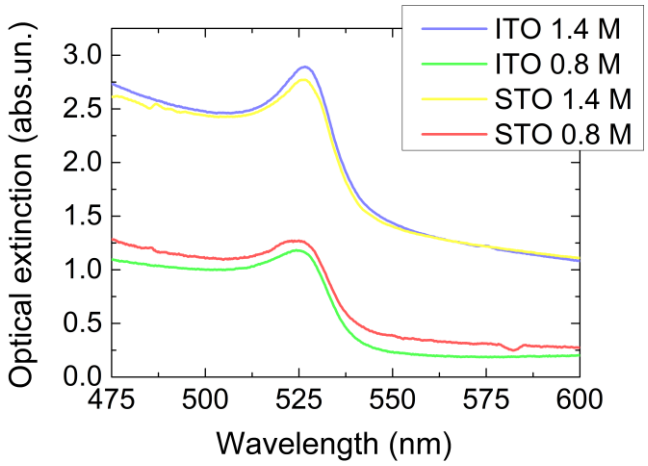

Figure S1. Optical absorption spectra obtained as average of the single spectra shown in Figure 1(a-d) in the main text, prior to the background subtraction.

S2 Characterization of the 0.4 M $MAPbBr_3$ film on STO

Figure S2 shows the analysis of a $MAPbBr_3$ film deposited on STO with 0.4 M precursor molarity. The characterization protocol of this sample was the same employed for the ones reported in the main text. The film thickness, obtained from the absorbance spectrum in Figure S2(a) was estimated around 40 nm.

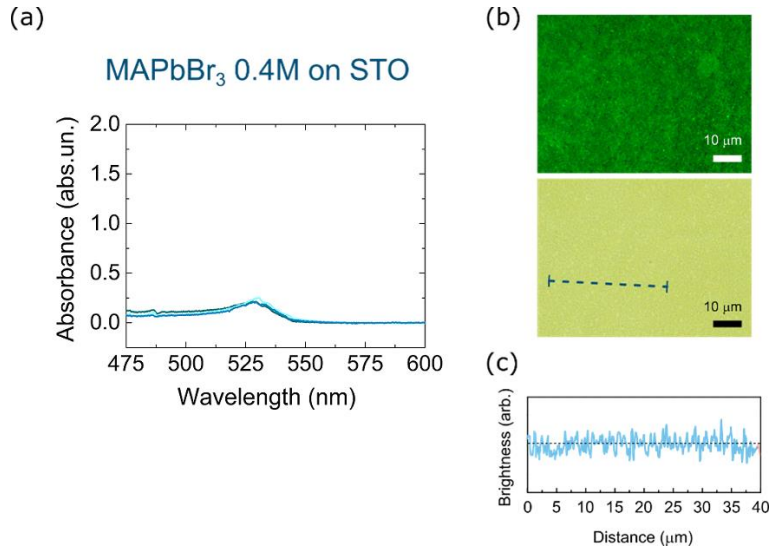

Figure S2. (a) Individual absorbance spectra acquired on three different sites of the $MAPbBr_3$ film deposited on STO at 0.4 M precursor (same scale as in Figure 1, panels a-d in the main text). (b) Fluorescence spectroscopy image (top) and optical microscopy image (bottom panel). (c) Film texture profile, extracted from dashed lines in panel b with Gwyddion software.

S3 Physical degradation of the 0.8 M $MAPbBr_3$ film on ITO stored in vacuum

Figure S3 shows the progressive physical degradation of a $MAPbBr_3$ film deposited on ITO with 0.8 M precursor molarity. Figure S3(a) shows the surface of the pristine sample. The film evenly covers the substrate surface, as observed even at the highest magnification. Figure S3(b) shows the film surface after 2 weeks of storage in vacuum atmosphere. Here, the bare surface of the ITO substrate (appearing in blue) is visible, as evidence that the physical degradation of the perovskite

film is quickly developing. Comparing to the images of the samples deposited with 1.4 M concentration (Figure 3(b, h) of the main text) physical degradation appears on a faster timescale, probably ascribed to the smaller amount of perovskite (thinner film) deposited in this sample. In Figure S4, we show an SEM image of the pristine 0.8 M HOIP film as deposited on ITO. The film appears rather compact, but a granular pattern in the morphology on a size scale ~300 nm is already visible (see arrows). We remark that the surface to volume ratio is higher for thinner samples, which are expected to degrade more quickly. Indeed, in this sample the ITO substrate is exposed from physical degradation already in the two weeks' timestamp, also resulting in the accumulation of the remaining HOIP layer in a larger amount of the compact crystallites. After three weeks of vacuum storage, the film has undergone complete physical degradation, as shown in Figure S3(c), and the perovskites microcrystals gather in clusters as a consequence of the contraction effect.

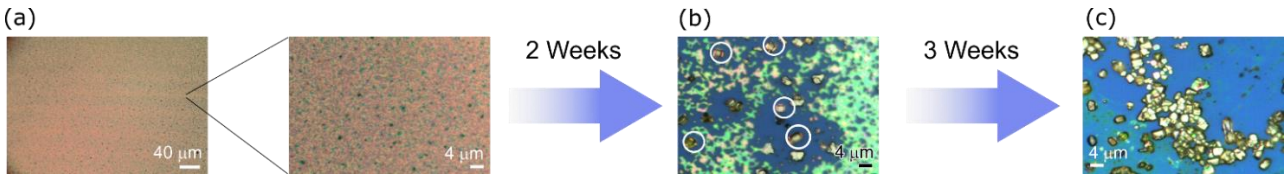

Figure S3. (a) Optical microscopy images of the $MAPbBr_3$ film deposited on ITO at 0.8M. (b) Acquisition of the images of the film stored in 13 mbar vacuum for two weeks, and (c) stored in 13 mbar vacuum for three weeks. Images were acquired with 20x and 100x magnification.

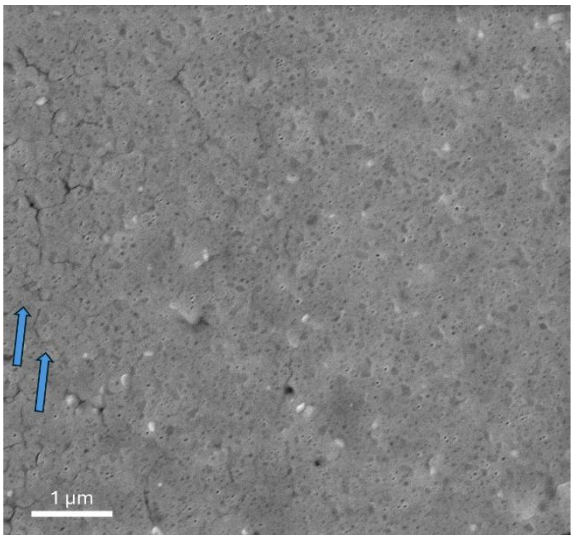

Figure S4. SEM image of the MAPbBr3 film deposited on ITO at 0.8M. The light blue arrows mark some grain boundaries already visible in the pristine sample on a scale of ~300 nm.

S4 Chemical degradation of the $MAPbBr_3$ film on STO

Figure S5(a,b) shows the $NH_4Pb_2Br_5$ aggregates formed on the 1.4 M $MAPbBr_3$ films deposited on STO (panel a) and ITO (panel b) after two weeks of storage under vacuum environment. On the STO substrate these aggregates appear as white regions on the surface, while for the one deposited on ITO, they are visible as purple spots. In Figure S5c the Raman spectrum at low frequencies acquired on these aggregates are reported and compared with that acquired on the $NH_4Pb_2Br_5$ crystals observed on the thinner sample reported in the main text.

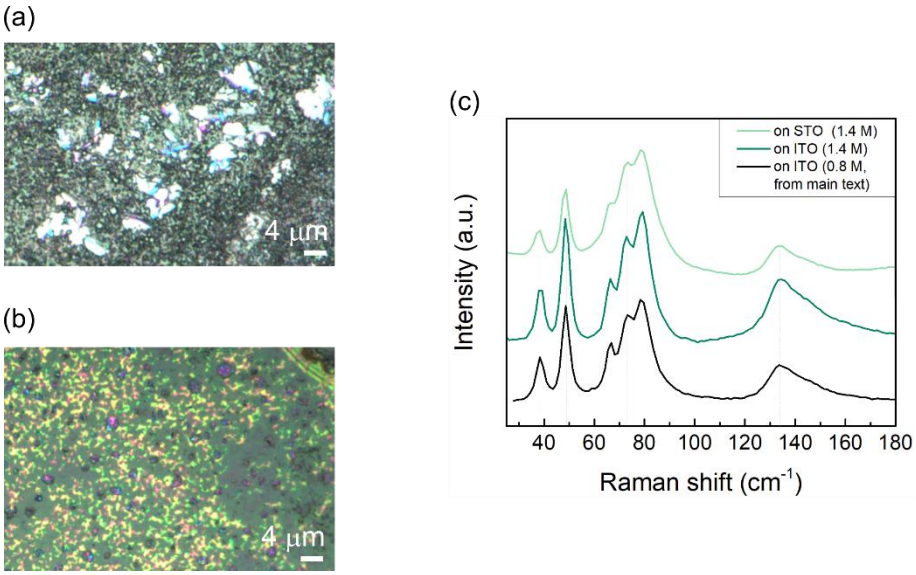

Figure S5. (a, b) Optical microscopy image of the 1.4 M $MAPbBr_3$ film on STO and ITO after two weeks of vacuum storage at 13 mbar, both acquired with 100x magnification. (c) Raman spectra of the aggregates at low Raman shift acquired on the sample on STO (black line), and ITO (green line).

S5 Proposed chemical reaction pathways for the formation of $NH_4Pb_2Br_5$

The formation of $NH_4Pb_2Br_5$ from $MAPbBr_3$ suggests the breaking of the C-N bond in the methylammonium cation, a step implying that the chemical reaction is favored in vacuum and is triggered by the presence of crystalline defects in the film. The chemical pathway here proposed is the following:

$$CH_3NH_3PbBr_{3\,(s)} \longrightarrow CH_3NH_{2\,(g)} + HBr_{(g)} + PbBr_{2\,(s)}$$

$$CH_3NH_{2\,(g)} + HBr_{(g)} \rightleftharpoons CH_3Br_{(g)} + NH_{3\,(g)}$$

$$NH_{3\,(g)} + HBr_{(g)} \longrightarrow NH_4Br_{(s)}$$

$$NH_4Br_{(s)} + 2\,PbBr_{2\,(s)} \longrightarrow NH_4Pb_2Br_{5\,(s)}$$

The first stage of this chain reaction, which foresees the degradation of the perovskite into methylamine (CH_3NH_2), hydrobromic acid (HBr), and lead bromide ($PbBr_2$) is a well-established degradation route for $MAPbX_3$ based perovskites.[R1,R2,R3] This reaction should not occur spontaneously at ambient temperature and atmospheric pressure [R3] but could in principle take place in low vacuum conditions, as the volatile products (CH_3NH_2 and HBr) can move away from the reaction environment thus shifting the reaction to the right. The second stage consists of a nucleophilic substitution leading to the breaking of the C-N bond and the formation of the two gaseous compounds CH_3Br and NH_3.[R4] Although ammonia is not commonly detected in the degradation of halide perovskites, prolonged storage in vacuum could have favored the process. Our hypothesis foresees that keeping the sample in vacuum could increase the tendency of methylamine (produced in the first stage of the degradation process) to desorb from the perovskite surface.[R5, R6] This could make the molecule more prone to react with HBr because this reaction is more thermodynamically favored.[R7] It has been patented that adding a certain amount of ammonia facilitates the stability of the solar cells: this corroborates the proposed reaction pathway, as ammonia is quasi-equivalent to the product of

methylammonium deprotonation and would prevent the volatilization of deprotonated methylammonium.

In the third stage of the reaction, a proton from the hydrogen halide HBr is transferred to the ammonia causing the formation of a NH_4Br salt. Finally, the last step of the degradation process provides for the reaction between a molecule of methylammonium bromide and two molecules of $PbBr_2$, giving the final experimentally observed product that is $NH_4Pb_2Br_5$.

A second degradation mechanism is also suggested for the formation of $NH_4Pb_2Br_5$ from $MAPbBr_3$. In this process, also favored by vacuum storage, ammonia is produced by a photocatalyzed radical reaction, [R8] which is possible given the films were not stored in the dark. The mechanism should be considered as a hypothesis which deserves further investigation, since no evidence of its intermediate gaseous products was detectable by optical methods. Since we believe this might be of applicative interest, particularly for the formulation of synthesis protocols, we report the process in the following:

$$MAPbBr_{3\ (s)} \xrightarrow{h\nu} MAPbBr_3^{*}{}_{(s)} \longrightarrow h^{+}_{VB-MAPbBr_3} + e^{-}_{CB-MAPbBr_3}$$

$$CH_3NH_{2\ (g)} \xrightarrow{MAPbBr_3^{*}{}_{(s)}} CH_3NH_2^{\cdot +}{}_{(g)} + MAPbBr_{3\ (s)} + e^{-}_{CB-MAPbBr_3}$$

$$CH_3NH_2^{\cdot +}{}_{(g)} \xrightarrow{-H^{+}} H_2\dot{C}-NH_{2\ (g)}$$

$$H_2\dot{C}-NH_{2\ (g)} \longrightarrow \ddot{C}H_{2\ (g)} + \dot{N}H_{2\ (g)}$$

$$\dot{N}H_{2\ (g)} \xrightarrow{e^{-}_{CB-MAPbBr_3}} NH_2^{-}{}_{(g)}$$

$$NH_2^{-}{}_{(g)} \xrightarrow{H^{+}} NH_{3\ (g)}$$

In this sequence of reactions, the $MAPbBr_3$ perovskite is firstly photoexcited and an electron is promoted from the valence band to the conduction band of the compound ($MAPbBr_3^{*}$). Afterwards, the excited electrons are transferred from the HOMO orbital of a methylamine molecule, already present in the lattice as a punctual defect (cation vacancy), to the valence band of the photo-excited

perovskite, which will be reduced in this way. The radical methylamine cation ($CH_3NH_2^{\cdot +}$) formed in the previous stage of the reaction, yields an acidic methyl proton (third stage), and then dissociates by homolytic scission of the C-N bond, forming a carbene ($:CH_2$), and the radical $NH_2^{\cdot}$ (fourth stage). Finally, an electron is transferred from the reduced $MAPbBr_3$ to the $NH_2^{\cdot}$ with the formation of the anion NH_2^- which protonates to produce ammonia. Similar to what happens in the first proposed degradation mechanism, ammonia reacts with a molecule of HBr via an acid-base reaction to create NH_4Br. The latter, in turn, reacts with $PbBr_2$ given by the structural collapse of the perovskite, to produce $NH_4Pb_2Br_5$.

References

R1. X. Wu, X. Zhang, W. Yu, Y. Zhou, W. Wong, W. He, K. P. Loh, X.-F. Jiang and Q.-H. Xu, *Journal of Materials Chemistry A*, 2023, **11**, 4292–4301.

R2. E. J. Juarez-Perez, L. K. Ono, M. Maeda, Y. Jiang, Z. Hawash and Y. Qi, *Journal of Materials Chemistry A*, 2018, **6**, 9604–9612.

R3. E. J. Juarez-Perez, L. K. Ono, I. Uriarte, E. J. Cocinero and Y. Qi, *ACS Applied Materials & Interfaces*, 2019, **11**, 12586–12593.

R4. B. Brunetti, C. Cavallo, A. Ciccioli, G. Gigli and A. Latini, *Scientific Reports*, 2016, **6**, 1–10.

R5. E. J. Juarez-Perez, Z. Hawash, S. R. Raga, L. K. Ono and Y. Qi, *Energy & Environmental Science*, 2016, **9**, 3406–3410.

R6. A. Alberti, I. Deretzis, G. Pellegrino, C. Bongiorno, E. Smecca, G. Mannino, F. Giannazzo, G. G. Condorelli, N. Sakai, T. Miyasaka et al., *ChemPhysChem*, 2015, **16**, 3064–3071.

R7. E. Smecca, Y. Numata, I. Deretzis, G. Pellegrino, S. Boninelli, T. Miyasaka, A. La Magna and A. Alberti, *Physical Chemistry Chemical Physics*, 2016, **18**, 13413–13422.

R8. M. Liu, J. Zhao, Z. Luo, Z. Sun, N. Pan, H. Ding and X. Wang, *Chemistry of Materials*, 2018, 30, 5846–5852.